arXiv:1409.0078v1 [cond-mat.supr-con] 30 Aug 2014

Multiband Te p Based Superconductivity of $Ta_4Pd_3Te_{16}$

David J. Singh
Materials Science and Technology Division, Oak Ridge National Laboratory, Oak Ridge, Tennessee 37831-6056
(Dated: September 2, 2014)

$Ta_4Pd_3Te_{16}$ is a recently discovered superconductor that has been suggested to be an unconventional superconductor near magnetism. We report electronic structure calculations showing that in spite of the layered crystal structure the material is an anisotropic three dimensional metal. The Fermi surface contains prominent one and two dimensional features, including nested 1D sheets, a 2D cylindrical section and a 3D sheet. The electronic states that make up the Fermi surface are mostly derived from Te p states, with small Ta d and Pd d contributions. This places the compound far from magnetic instabilities. The results are discussed in terms of multiband superconductivity.

PACS numbers: 74.20.Rp,74.20.Pq,74.70.Dd

I. INTRODUCTION

Jiao and co-workers recently discovered superconductivity with a critical temperature T_c=4.6 K in $Ta_4Pd_3Te_{16}$.[1] These authors concluded that there is evidence for strong electron-electron interactions in this compound based on an analysis of the specific heat. Moreover, Pan and co-workers reported that T_c increases to over 6 K under pressure and found a linear contribution to the temperature dependent thermal conductivity, which increases with magnetic field similar to cuprate superconductors.[2] This implies an electronic thermal conductivity contribution in the superconducting phase, i.e. line nodes or some part of the Fermi surface that is not gapped. These measurements, which extend to T=80 mK, which is well below T_c, were taken as implying an unconventional superconducting state, perhaps associated with the quasi-one-dimensional features of the crystal structure.[2]

The crystal structure (Fig. 1) shows a layered structure with Ta and Pd atoms occurring in one dimensional chains. The structure differs from those of the superconducting chalcogenides Ta_2PdS_5, $Nb_2Pd_{0.8}S_5$ and $Nb_3Pd_{0.7}Se_7$ in being a stoichiometric compound with nominally flat two dimensional sheets in the crystal structure.[3–6] We note that there is the possibility that the layered crystal structure may be misleading from the point of view of the electronic properties, as previous electronic structure calculations by Alemany and co-workers showed important interlayer Te – Te interactions.[7] In addition, it should be noted that there are considerable local distortions around the different Te atoms in the structure. Here we report electronic structure calculations in relation to the above observations.

II. METHODS

The calculations reported here were performed using standard density functional theory with the generalized gradient approximation of Perdew, Burke and Ernzerhof (PBE-GGA).[8] We used the general potential linearized augmented planewave (LAPW) method[9] as implemented in the WIEN2k code.[10] We used well converged LAPW basis sets plus local orbitals to treat the semicore states. The LAPW sphere radii were R=2.5 bohr for all atoms, and the planewave sector cutoff, k_{max} was set according to Rk_{max}=9.

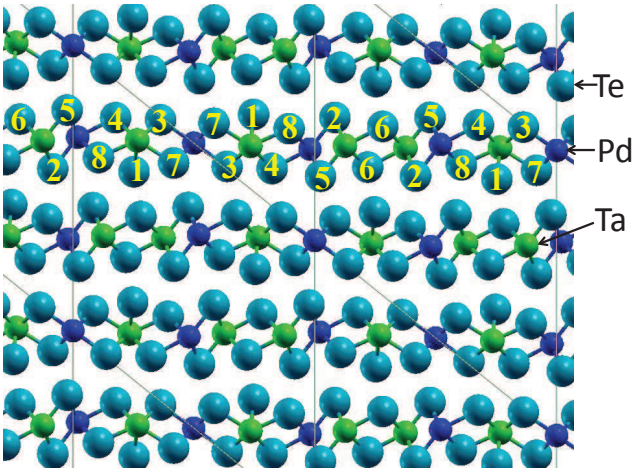

FIG. 1. (color online) Crystal structure of $Ta_4Pd_3Te_{16}$ viewed along the c-axis (in spacegroup 12, $C2/m$, setting 2, unique axis c). The unit cell is indicated by the lines. The atomic positions are from the total energy minimization. The Te atoms in one layer are labeled according to the inequivalent Te positions in the structure (see text).

The monoclinic lattice parameters were taken from the experimental data of Mar and Ibers,[11] a=21.2762 Å, b=19.510 Å, c=3.735 Å, γ=128.825° (note we show results using spacegroup 12, $C2/m$ setting 2, unique axis c, while the original paper of Mar and Ibers uses setting 1, unique axis b). The internal atomic coordinates were then determined by total energy minimization with the PBE-GGA starting from the experimental structure including relativity at the scalar relativistic level for the valence bands. The resulting structure, shown in Fig. 1, was used for the electronic structure calculations. These were performed self-consistently including spin-orbit for all states. The shortest Te – Te distance that couples

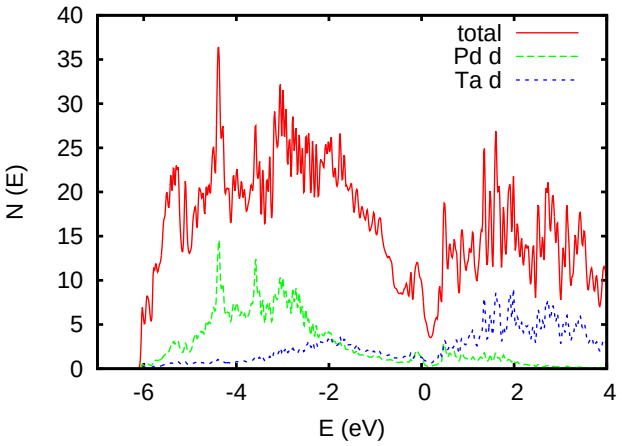

FIG. 2. (color online) Calculated electronic density of states and projections of Pd d and Ta d character on a per formula unit basis. The Fermi energy is at 0 eV.

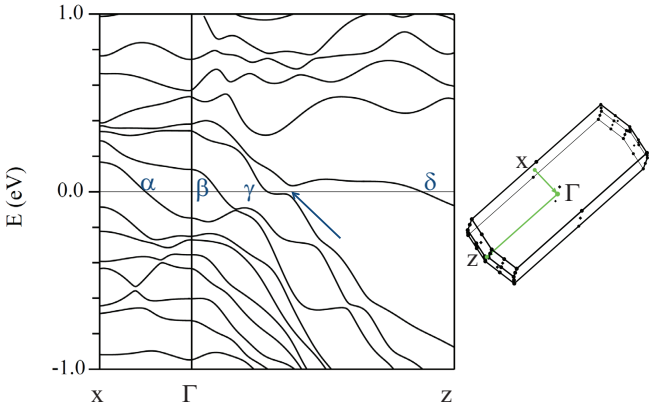

FIG. 3. (color online) Band structure of $Ta_4Pd_3Te_{16}$ along the lines shown in the right panel. The band crossings corresponding to the four sheets of Fermi surface are labeled with Greek letters. The arrow denotes the anticrossing as discussed in the text. The Fermi energy is at 0 eV.

different layers in the relaxed structure is 3.61 Å, which is short enough for significant interlayer Te – Te interactions, as were discussed by Alemany and co-workers.[7]

The relaxed structure (Fig. 1) is quite complex as seen. In particular, while nominally the structure could be described as Te bilayers with metal atoms in the interstitial sites, it is clear that these bilayers are very strongly distorted. These distortions lead to interesting structural features, such as short bonded Te zig-zag chains along the c-axis composed of the Te1 and Te8 atoms, as labeled in the figure, with a Te-Te bond length of only 3.22 Å. Also, there are large differences between the different Te sites. The nearest Te-Te distances for the different Te atoms run from 3.08 Å, for the Te3-Te4 bond, to 3.73 Å, for Te2. Also the bond valence sums are far from the nominal value and vary among the different Te, ranging from 2.68 (Te7) to 2.91 (Te8). This implies an important role for Te-Te bonding. The experimentally reported crystal structure refinement[11] shows similar features including both the range of Te-Te bond lengths and the variation in bond valence sums. While this is unusual, it is reminiscent of $IrTe_2$, which shows a first order structural transition related to frustrated Te-Te p bonding.[12,13]

III. ELECTRONIC STRUCTURE

The calculated electronic density of states and projections of Pd d and Ta d character are shown in Fig. 2. There is strong hybridization between both types of metal atoms and the Te evident in this plot. The Ta and Pd d contributions occur in broad peaks above and below the Fermi level, E_F. As seen, the Pd d orbitals are mostly occupied, while the Ta d orbitals are mostly unoccupied. In a fully ionic picture, one might assign valences Ta^{+5}, Pd^{+4} in order to obtain the correct stoichiometry with Te^{-2} However Pd^{4+}, would seem to be a highly unlikely valence especially in a telluride. The Pd density of states with its nearly fully occupied d orbitals below E_F is clearly not consistent with a Pd^{4+} state. Therefore important Te-Te p bonding is expected, consistent with that seen in the density of states.

The calculated value at the Fermi energy is $N(E_F)$=9.6 eV^{-1} per formula unit, which is significantly higher than the value of 5.5 eV^{-1} obtained by Alemany and co-workers.[7] We did calculations for the unrelaxed atomic coordinates[11] as well. However, and find a value similar to but slightly higher than the value with the relaxed structure. All results shown here are with the relaxed structure. The bare linear specific heat coefficient from our calculation is 22.7 mJ/(mol K^2). Comparing with the experimental value of 42.8 mJ/(mol K^2), one infers an enhancement of $(1+\lambda_{tot})$=1.89 or λ_{tot}=0.89, i.e. an intermediate coupling value. Importantly, as seen from the projections of the density of states, there is very little transition metal contribution to $N(E_F)$, which instead derives from Te p states. The Pd d contribution to $N(E_F)$ based on projection onto the Pd LAPW spheres is 1.3 eV^{-1} summed over the three Pd atoms, while the Ta contribution is similar at 1.3 eV^{-1} summed over the four Ta atoms. This strongly argues against nearness to magnetism in this compound.

The band structure in the range around the Fermi energy, E_F is given in Fig. 3. As shown, there are four bands crossing E_F, labeled in the plot. These give rise to four sheets of Fermi surface as depicted in Fig. 4. The are a 2D hole cylinder ("α"), two very 1D and therefore nested sheets ("β" and "γ")), which may lead to nearness to density wave instabilities, and a heavy 3D sheet ("δ"). The 2D cylinder, α, and the first 1D sheet, β anticross making the shapes of these surfaces more complex. Nonetheless the nesting is at $\sim 0.1\ 2\pi/c$ (from β) and $\sim 0.3\ 2\pi/c$ (from γ), i.e. along the direction of the metal chains. The contributions to $N(E_F)$ from these are 1.4 eV^{-1}, 1.8 eV^{-1}, 1.0 eV^{-1} and 5.4 eV^{-1}, for sheets α,

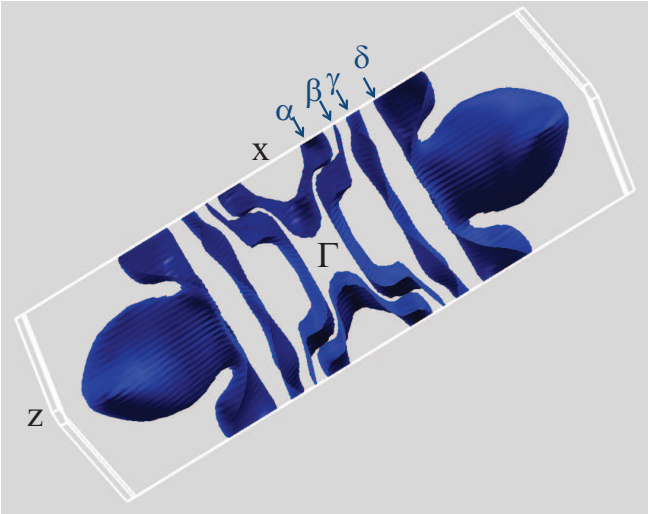

FIG. 4. (color online) Fermi surface $Ta_4Pd_3Te_{16}$. The four sheets are labeled corresponding to the bands in Fig. 3.

β, γ and δ, respectively, following the labels of Fig. 3. In addition, there is an anticrossing with another Te p derived band very close to the Fermi energy crossing of γ as indicated by the arrow in Fig. 3. This would come to the Fermi energy for very small levels of hole doping. Such hole doping could come from Ta deficiency. We emphasize that as is evident from the density of states, all of these sheets of Fermi surface are derived from Te p states and there is little transition element d character at the Fermi energy. This implies that any nearby density wave instability due to nesting would be a charge density wave (CDW) and not a spin density wave (SDW). This density wave, if it actually condensed, would consist of a structural modulation along the short c-axis, metal chain direction, which should be clearly seen in diffraction.

The mixture of 1D-like, 2D-like and 3D Fermi surfaces leads to a net anisotropic, but 3D metal. The conductivity anisotropy was estimated by integrating the transport function σ/τ, where τ is the scattering rate, taken as constant for all bands and directions. The eigenvalues of the σ/τ tensor are 3.9 x 10^{19} $(\Omega\ \mathrm{m\ s})^{-1}$, 1.5 x 10^{19} $(\Omega\ \mathrm{m\ s})^{-1}$ and 10.5 x 10^{19} $(\Omega\ \mathrm{m\ s})^{-1}$, with directions approximately (note the monoclinic symmetry) in the layers, perpendicular to c, approximately across the layers, and along c, respectively. As noted, the nesting feature is along the c-axis direction. This means that if a density wave condensed, or if there were strong scattering associated with soft phonons related to the nesting, this would primarily affect the nested sheets, and therefore the c-axis direction conductivity.

We now turn to the details of the band structure. Because of the low symmetry, the different bands have mixed orbital and atomic character. The following is a description of the main characters. The 2D α sheet is derived from a mixture of different Te p states, and of the four sheets is the sheet with the most Ta d character. The 1D β as mainly Te7 (Fig. 1) character. This is similar to the other 1D (γ) sheet, which in addition involves Te1 and Te5 orbitals. The 3D, δ sheet, which is the sheet that makes the largest contribution to $N(E_F)$ is mainly from Te3 p-orbitals, which are hybridized with Pd d states. Thus the different sheets of Fermi surface, and in particular the nested quasi-1D sheets and the other sheets are associated with different orbitals on different atoms.

IV. DISCUSSION AND CONCLUSIONS

As mentioned, $Ta_4Pd_3Te_{16}$ is a low temperature superconductor, with experimental signatures of possible unconventional behavior. One such signature is an inconsistency between the superconducting λ_{sc} inferred from the specific heat jump, which implies weak coupling behavior, and that inferred from the enhancement of the low temperature specific heat, $\gamma = \gamma_{bare}(1 + \lambda_{tot})$.[1] In particular, Jiao and co-workers measured the specific heat jump as $\Delta C/(\gamma T)$=1.4 $\pm$ 0.2 consistent with the weak coupling BCS value of 1.43, implying low λ_{sc}. This included a careful correction for the superconducting volume fraction. They also inferred λ_{tot}=2.3 by combining the measured specific heat γ with density of states $N(E_F)$=5.5 eV^{-1} from the report of Alemany and co-workers.[7] However, we obtain a higher $N(E_F)$=9.6 eV^{-1}, which then gives a correspondingly lower renormalization and λ_{tot}=0.89. This is quite reasonable considering the specific heat jump. Therefore it may not be necessary to consider an enhancement to λ_{tot} due to non-phonon channels such as spin fluctuations to reconcile the γ with the specific heat jump.

We note that the transition metal d contribution to $N(E_F)$ is low, which argues against spin-fluctuations. Also, it should be noted that the Fermi surface consists of four distinct sheets with contributions from different atoms. Therefore it is reasonable to expect that the pairing interactions could be stronger on some sheets than others, which would complicate the simple interpretation of the specific heat jump using a single band BCS formula.

From the point of view of superconductivity, nearness to a CDW can provide an attractive interaction through the electron phonon interaction. If this is the main pairing interaction the gap would be largest on the nested Fermi surface sheets. This type of interaction favors a singlet state and unless there is an additional repulsive interaction, such as spin-fluctuations or a strong Coulomb repulsion, will not lead to a state with any sign changes in the order parameter. Spin fluctuations associated with nearness to an SDW resulting from the nested 1D sheets could lead to a specific heat enhancement, i.e. a larger λ_{tot}, as discussed by Jiao and co-workers.[1] As mentioned, this may not be needed considering the value of the bare $N(E_F)$ from our calculations. In any case, such an interaction cannot lead to superconductivity on the nested

sheets with the Fermi surface structure of this compound. The reason is that in a singlet channel, spin fluctuations are repulsive, which would favor an order parameter that changes sign between the nested sheets on opposite sides of the zone center, i.e. a triplet state, while in a triplet channel spin fluctuations are attractive, which would favor an order parameter that is the same on opposite sides of the zone center, i.e. not a triplet. Besides the possibility of pairing due to nearness to a CDW, it is to be noted that there are other layered tellurides, in particular $Ir_{1-x}Pt_xTe_2$ that become superconducting[14] and which do not have Fermi surface nesting features that lead to phonon softening.[13] Thus it may well be that $Ta_4Pd_3Te_{16}$ is also an s-wave superconductor with pairing from phonons associated with the Te-Te p bonding and a Fermi surface associated Te p bands.

Recently, Pan and co-workers reported thermal conductivity measurements on a single crystal sample with a low residual resistivity below 4 $\mu\Omega$ cm. They found a large linear electronic contribution persisting down to T=80 mK, and furthermore that this contribution increases with field similar to the behavior of a cuprate superconductor. This implies the presence of ungapped parts of the Fermi surface, such as line nodes. The data are reminiscent of cuprates and also certain of the Fe-based superconductors, for which there is other evidence of line nodes.[15] The observed behavior is inconsistent with the behavior of the two gap superconductor $NbSe_2$. On the other hand, it could be compatible with a clean multigap superconductor where the gap ratio is larger, and in fact that data has some similarity to MgB_2,[16] which is an s-wave electron phonon superconductor. Considering the magnitude of the linear thermal conductivity seen experimentally and using the Wiedemann-Franz relation, one would have to assume that parts of Fermi surface contributing $\sim$ 30% of the conductivity have very small gaps, in order to explain the data without line nodes. This is possible considering the Fermi surface structure, in which several different sheets contribute to the conductivity and to $N(E_F)$. The fact that these sheets derive from p states associated with different Te atoms makes more plausible large differences in the coupling on different sheets, which may then lead to large differences in the gaps for a clean sample.

It will be of interest to study samples with higher levels of disorder in order to distinguish these two possibilities. Specifically, with line nodes, disorder is expected to suppress the ordering temperature, while in the multiband case disorder would enhance the gap on the low gap parts of the Fermi surface and thereby suppress the electronic thermal conductivity at low temperature. Also, we note that the electronic thermal conductivity has the same anisotropy as the electronic conductivity from the ungapped parts of the Fermi surface. We find sheets with very different anisotropies, 1D sheets, a 2D sheet and a 3D sheet. Therefore, in a scenario in which there is a small gap on some part, the particular sheets involved in the electronic thermal conductivity (i.e. the low gap sheets) could be identified from the anisotropy of the electronic part of the thermal conductivity in the superconducting state.

To summarize, electronic structure calculations for $Ta_4Pd_3Te_{16}$ show four sheets of Fermi surface derived primarily from Te p states. Importantly, the transition metal contribution to the density of states is too low to place the system near magnetism. The calculated value of $N(E_F)$=9.6 eV^{-1} is higher than that from a prior calculation[7], which can resolve a discrepancy between the specific heat jump and the specific heat renormalization. The Fermi surface includes nested 1D-like sections, a 2D-like section and a heavy 3D section, which makes the largest contribution to $N(E_F)$. The net result is a rather anisotropic but 3D metal. Thus $Ta_4Pd_3Te_{16}$ is a multiband superconductor with an electronic structure derived mostly from Te p states.

ACKNOWLEDGMENTS

This work was supported by the U.S. Department of Energy, Basic Energy Sciences, Materials Sciences and Engineering Division.

[1] W. H. Jiao, Z. T. Tang, Y. L. Sun, Y. Liu, Q. Tao, C. M. Feng, Y. W. Zeng, Z. A. Xu, and G. H. Cao, J. Am. Chem. Soc. **136**, 1284 (2014).
[2] J. Pan, W. H. Jiao, X. C. Hong, Z. Zhang, L. P. He, P. L. Cai, J. Zhang, G. H. Cao, and S. Y. Li, cond-mat , arXiv:1404.0371 (2014).
[3] Q. R. Zhang, D. Rhodes, B. Zeng, T. Besara, T. Siegrist, M. D. Johannes, and L. Balicas, Phys. Rev. B **88**, 024508 (2013).
[4] Q. Zhang, G. Li, D. Rhodes, A. Kiswandhi, T. Besara, B. Zeng, J. Sun, T. Siegrist, M. D. Johannes, and L. Balicas, Sci. Rep. **3**, 1446 (2013).
[5] Y. F. Lu, T. Takayama, A. F. Bangura, Y. Katsura, D. Hashizume, and H. Takagi, J. Phys. Soc. Jpn. **83**, 023702 (2014).
[6] D. J. Singh, Phys. Rev. B **88**, 174508 (2013).
[7] P. Alemany, S. Jobic, R. Brec, and E. Canadell, Inorg. Chem. **36**, 5050 (1997).
[8] J. P. Perdew, K. Burke, and M. Ernzerhof, Phys. Rev. Lett. **77**, 3865 (1996).
[9] D. J. Singh and L. Nordstrom, *Planewaves Pseudopotentials and the LAPW Method, 2nd Edition* (Springer, Berlin, 2006).
[10] P. Blaha, K. Schwarz, G. Madsen, D. Kvasnicka, and J. Luitz, WIEN2k, An Augmented Plane Wave + Local Orbitals Program for Calculating Crystal Properties (K. Schwarz, Tech. Univ. Wien, Austria) (2001).

[11] A. Mar and J. A. Ibers, J. Chem. Soc., Dalton Trans. **1991**, 639 (1991).
[12] A. F. Gang, G. Xu, T. Dong, P. Zheng, and N. L. Wang, Sci. Rep. **3**, 1153 (2013).
[13] H. Cao, B. C. Chakoumakos, X. Chen, J. Yan, M. A. McGuire, H. Yang, R. Custelcean, H. Zhou, D. J. Singh, and D. Mandrus, Phys. Rev. B **88**, 115122 (2013).
[14] S. Pyon, K. Kudo, and M. Nohara, J. Phys. Soc. Jpn. **81**, 053701 (2012).
[15] K. Hashimoto, M. Yamashita, S. Kasahara, Y. Senshu, N. Nakata, S. Tonegawa, K. Ikada, A. Serafin, A. Carrington, T. Terashima, H. Ikeda, T. Shibauchi, and Y. Matsuda, Phys. Rev. B **81**, 220501 (2010).
[16] A. V. Sologubenko, J. Jun, S. M. Kazakov, J. Karpinski, and H. R. Ott, Phys. Rev. B **66**, 014504 (2002).